

Spectral, Thermal and Raman Analysis of Dy³⁺ Doped Borosilicate Glasses with Large Thermal Stability Parameter

S.L.Meena

Ceramic Laboratory, Department of physics, Jai Narain Vyas University, Jodhpur 342001(Raj.) India

Abstract

Glass sample of yttrerbium zinc lithium sodalimealumino borosilicate(25-x)SiO₂:10ZnO:10Li₂O:10Na₂O:10K₂O:10Al₂O₃:10Yb₂O₃:15B₂O₃:xDy₂O₃(wherex=1,1.5 and 2 mol%) have been prepared by melt-quenching technique. The amorphous nature of the prepared glasssamples was confirmed by X-ray diffraction. Optical absorption,excitation spectrum, fluorescence and raman spectra were recorded at roomtemperature for all glass samples.Judd-Ofeltintensity parameters Ω_{λ} ($\lambda=2, 4$ and 6) are evaluated from theintensities of various absorption bands of opticalabsorption spectra. Using these intensity parameters variousradiative properties like spontaneous emission probability, branching ratio, radiative life time and stimulatedemission cross-section of various emission lines have been evaluated

Keywords: YZLSLABS Glasses,Raman Analysis,Optical Properties, Judd-Ofelt Theory, Thermal properties.

Date of Submission: 14-09-2025

Date of acceptance: 28-09-2025

I. Introduction

Glasses doped with trivalent rare earth doped are very important due to its potential applications in areas such as optical amplifications,photoelectronic device,optical data storage, andsolid state lasers[1-5]. Among different glasses, silicate glasses have unique properties. They have high refractive index, high transparency and high thermal stability. Borosilateglasses possess interesting properties like high solubility,low melting temperature,lower phonon energy, high gain densityandnon-linear optical susceptibilities[6-11].Glasses containing heavy metal oxides exhibits good chemical durability and non-linear optical properties [12-14].ZnO is also added due to its specific chemical and physical properties.Boric acid acts as a good glass former and flux material.B₂O₃ glass network could significantly improve different properties like mechanical strength and thermal stability. The addition of oxide such as Li₂O and Al₂O₃ are used for improves the chemical durability of glasses[15-17].The high thermal stability, low glass melting temperature and good rare earth ion solubility makes the borosilateglasses suitable candidates for photonic applications[18-20].Recently Dy³⁺ ions doped glasses found important in the area laser action and Thermionic applications [21-24].

The present work reports on the preparation and characterization of rare earth doped heavy metal oxide (HMO) glass systems for lasing materials.I have studied on the absorption,excitation, fluorescence and raman spectraof Dy³⁺doped yttrerbium zinc lithium sodalimealumino borosilicate glasses. The intensities of the transitions for the rare earth ions have been estimated successfully using the Judd-Ofelt theory, The laser parameters such as radiative probabilities(A),branching ratio (β),radiative life time(τ_R) and stimulated emission cross section(σ_p) are evaluated using J.O.intensity parameters(Ω_{λ} , $\lambda=2,4$ and 6).The network structure of the formed glass system were studied using raman spectra.

II.Experimental Techniques

Preparation of glasses

The following Dy³⁺doped borosilicate glass samples (25-x)SiO₂:10ZnO:10Li₂O:10Na₂O:10K₂O:10Al₂O₃:10Yb₂O₃:15B₂O₃:xDy₂O₃ (where x=1,1.5 and 2 mol%) have been prepared by melt-quenching method. Analytical reagent grade chemical used in the present study consist of SiO₂,ZnO,Li₂O, Na₂O,K₂O,Al₂O₃,Yb₂O₃,B₂O₃and Dy₂O₃. They were thoroughly mixed by using an agate pestle mortar. then melted at 980°C by an electrical muffle furnace for 2h., After complete melting, the melts were quickly poured in to a preheated stainless steel mould and annealed at temperature of 350°C for 2h to remove thermal strains and stresses. Every time fine powder of cerium oxide was used for polishing the samples. The

glass samples so prepared were of good optical quality and were transparent. The chemical compositions of the glasses with the name of samples are summarized in **Table 1**.

Table 1.

Chemical composition of the glasses

Sample	Glass composition (mol %)
YZLSLABS (UD)	25SiO ₂ :10ZnO:10Li ₂ O:10Na ₂ O:10K ₂ O:10Al ₂ O ₃ :10Yb ₂ O ₃ :15B ₂ O ₃
YZLSLABSDY(1.0)	24SiO ₂ :10ZnO:10Li ₂ O:10Na ₂ O:10K ₂ O:10Al ₂ O ₃ :10Yb ₂ O ₃ :15B ₂ O ₃ :1.0 Dy ₂ O ₃ .
YZLSLABSDY(1.5)	23.5SiO ₂ :10ZnO:10Li ₂ O:10Na ₂ O:10K ₂ O:10Al ₂ O ₃ :10Yb ₂ O ₃ :15B ₂ O ₃ :1.5 Dy ₂ O ₃ .
YZLSLABSDY(2.0)	23SiO ₂ :10ZnO:10Li ₂ O:10Na ₂ O:10K ₂ O:10Al ₂ O ₃ :10Yb ₂ O ₃ :15B ₂ O ₃ :2.0Dy ₂ O ₃ .

YZLSLABS (UD) -Represents undopedYttrerbium Zinc Lithium SodalimeAlumino Borosilicate glass specimens.

YZLSLABS (DY)-Represents Dy³⁺dopedYttrerbium Zinc Lithium SodalimeAlumino Borosilicate glass specimens.

III.Theory

3.1Oscillator Strength

The intensity of spectral lines are expressed in terms of oscillator strengths using the relation [25].

$$f_{\text{expt.}} = 4.318 \times 10^{-9} \int \epsilon(\nu) d\nu \quad (1)$$

where, $\epsilon(\nu)$ is molar absorption coefficient at a given energy ν (cm⁻¹), to be evaluated from Beer–Lambert law. Under Gaussian Approximation, using Beer–Lambert law, the observed oscillator strengths of the absorption bands have been experimentally calculated [26], using the modified relation:

$$P_m = 4.6 \times 10^{-9} \times \frac{1}{cl} \log \frac{I_0}{I} \times \Delta\nu_{1/2} \quad (2)$$

where c is the molar concentration of the absorbing ion per unit volume, l is the optical path length, $\log I_0/I$ is optical density and $\Delta\nu_{1/2}$ is half band width.

3.2. Judd-Ofelt Intensity Parameters

According to Judd[27] and Ofelt[28] theory, independently derived expression for the oscillator strength of the induced forced electric dipole transitions between an initial J manifold $|4f^N(S, L) J\rangle$ level and the terminal J' manifold $|4f^N(S', L') J'\rangle$ is given by:

$$\frac{8\pi^2 m c \bar{\nu}}{3h(2J+1)n} \left[\frac{(n^2+2)^2}{9} \right] \times S(J, J') \quad (3)$$

Where, the line strength $S(J, J')$ is given by the equation

$$S(J, J') = e^2 \sum \Omega_\lambda \langle 4f^N(S, L) J \| U^{(\lambda)} \| 4f^N(S', L') J' \rangle^2 \quad (4)$$

$\lambda = 2, 4, 6$

In the above equation m is the mass of an electron, c is the velocity of light, $\bar{\nu}$ is the wave number of the transition, h is Planck's constant, n is the refractive index, J and J' are the total angular momentum of the initial and final level respectively, Ω_λ ($\lambda=2, 4$ and 6) are known as Judd-Ofelt intensity parameters.

3.3Radiative Properties

The Ω_λ parameters obtained using the absorption spectral results have been used to predict radiative properties such as spontaneous emission probability (A) and radiative life time (τ_R), and laser parameters like fluorescence branching ratio(β_R) and stimulated emission cross section (σ_p).

The spontaneous emission probability from initial manifold $|4f^N(S', L') J'\rangle$ to a final manifold $|4f^N(S, L) J\rangle$ is given by:

$$A[(S', L') J'; (S, L) J] = \frac{64 \pi^2 \bar{\nu}^3}{3h(2J'+1)} \left[\frac{n(n^2+2)^2}{9} \right] \times S(J', J) \quad (5)$$

Where, $S(J', J) = e^2 [\Omega_2 \| U^{(2)} \|^2 + \Omega_4 \| U^{(4)} \|^2 + \Omega_6 \| U^{(6)} \|^2]$

The fluorescence branching ratio for the transitions originating from a specific initial manifold $|4f^N(S', L') J' \rangle$ to a final many fold $|4f^N(S, L) J \rangle$ is given by

$$\beta[(S', L') J'; (S, L) J] = \frac{A[(S', L') J' \rightarrow (S, L) J]}{\sum_{\bar{S}, \bar{L}} A[(S', L') J' \rightarrow (\bar{S}, \bar{L}) J]} \quad (6)$$

S, L, J

where, the sum is over all terminal manifolds.

The radiative life time is given by

$$\tau_{\text{rad}} = \sum_{S, L, J} A[(S', L') J'; (S, L) J] = A_{\text{Total}}^{-1} \quad (7)$$

S, L, J

where, the sum is over all possible terminal manifolds. The stimulated emission cross-section for a transition from an initial manifold $|4f^N(S', L') J' \rangle$ to a final manifold $|4f^N(S, L) J \rangle$ is expressed as

$$\sigma_p(\lambda_p) = \left[\frac{\lambda_p^4}{8\pi c n^2 \Delta\lambda_{\text{eff}}} \right] \times A[(S', L') J'; (\bar{S}, \bar{L}) J] \quad (8)$$

where, λ_p the peak fluorescence wavelength of the emission band and $\Delta\lambda_{\text{eff}}$ is the effective fluorescence line width.

IV. Result and Discussion

4.1 XRD Measurement

Figure 1 presents the XRD pattern of the sample contain $-\text{SiO}_2$ which is show no sharp Bragg's peak, but only a broad diffuse hump around low angle region. This is the clear indication of amorphous nature within the resolution limit of XRD instrument

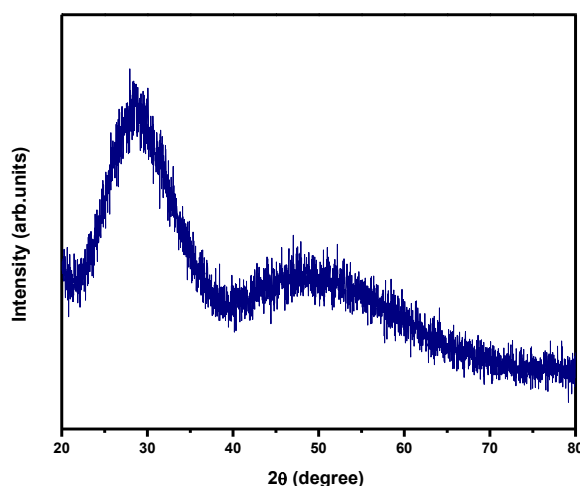


Fig.(1): X-ray diffraction pattern of YZLSLABS DY (1.0) glass.

4.2 Thermal Property

Differential thermal analysis checks the heat absorbed by glass samples during heating or cooling. Fig. 2 depicts the DTA thermogram of powdered YZLSLABS DY (1.0) sample. The glass transition temperature (T_g), onset crystallization temperature (T_c), crystallization temperature (T_p), melting temperature (T_m), thermal stability (T_s), Balaji Parameter (B_p), Hurbe's criterion (H_R) and reduced glass transition temperature (T_{rg}) were calculated. Shankar's parameter also calculated by using eq.(12). All the determined thermal parameters are given in table 2.

Table 2: Thermal stability parameters obtained from DTA curve of Dy³⁺ ions in YZLSLABS glasses.

Glass samples	T _g (°C)	T _c (°C)	T _p (°C)	T _m (°C)	T _s (°C)	B _p (°C)	H _R (°C)	K _s (°C)	T _{rg} (°C)
YZLSLABS DY(1.0)	376	508	547	686	132	3.385	0.742	34.251	0.548
YZLSLABS DY(1.5)	380	511	549	688	131	3.447	0.740	33.702	0.552
YZLSLABS DY(2.0)	382	512	555	693	129	3.000	0.713	33.693	0.551

The thermal stability of the glass samples can be calculated by difference between onset crystallization temperature and transition temperature [29].

$$\text{Thermal stability (T}_s\text{)} = T_c - T_g \quad (9)$$

Balaji Parameter can be calculated using [30].

$$\text{Balaji Parameter (B}_p\text{)} = [(T_c - T_g)/(T_p - T_c)]$$

Hruby's criterion is calculated using the Hruby's relation [31].

$$\text{Hruby's criterion (H}_R\text{)} = [(T_p - T_c)/(T_m - T_c)] \quad (10)$$

Reduced glass transition temperature is given as [32].

$$\text{Reduced glass transition temperature (T}_{rg}\text{)} = T_g/T_m \quad (11)$$

Thermal stability parameter can be calculated using formula.

$$\text{Thermal stability parameter (K}_s\text{)} = [(T_m - T_c) \times (T_c - T_g)] / T_m \quad (12)$$

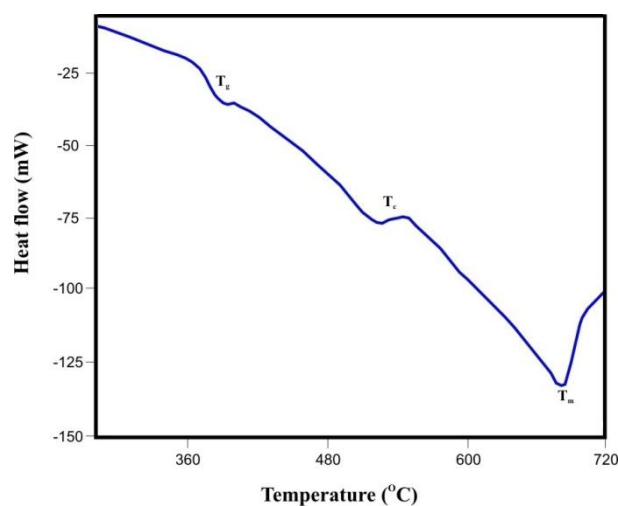


Fig.(2): DTA curve of YZLSLABS DY (1.0) glass.

4.3 Raman spectra

The Raman spectrum of Ytterbium Zinc Lithium SodaliAlumino Borosilicate (YZLSLABS DY-1.0) glass specimens is recorded and is shown in Fig. 3. The spectrum peaks located at 600, 795 and 1206 cm⁻¹. The band at 600 and 795 cm⁻¹ assigned to Si–O–Si symmetric stretching and bending vibration, respectively. The band at 1206 cm⁻¹ assigned to Si–O–Si asymmetric stretching.

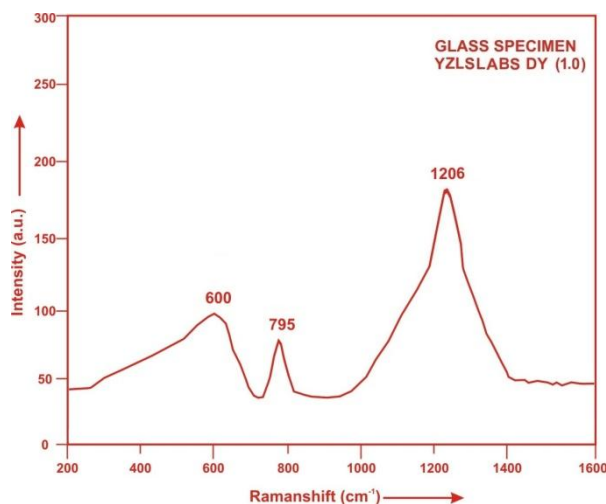


Fig. (3): Raman spectrum of YZLSLABS DY (1.0) glass.

4.4 Absorption Spectrum

The absorption spectra of Dy^{3+} -doped YZLSLABSDY (1.0) glass specimens have been presented in Figure 4 in terms of Intensity versus wavelength. Thirteen absorption bands have been observed from the ground state $^6H_{15/2}$ to excited states $^6H_{13/2}$, $^6H_{11/2}$, $^6H_{9/2}+^6F_{11/2}$, $^6H_{7/2}+^6F_{9/2}$, $^6F_{7/2}+^6H_{5/2}$, $^6F_{5/2}$, $^6F_{3/2}$, $^6F_{9/2}$, $^4I_{15/2}$, $^4G_{11/2}$, $^6F_{7/2}+^4I_{13/2}$, $^6M_{19/2}+4(P,D)_{3/2}$ and $^4G_{9/2}+^6P_{3/2}$ for Dy^{3+} -doped YZLSLABSDY (1.0) glasses.

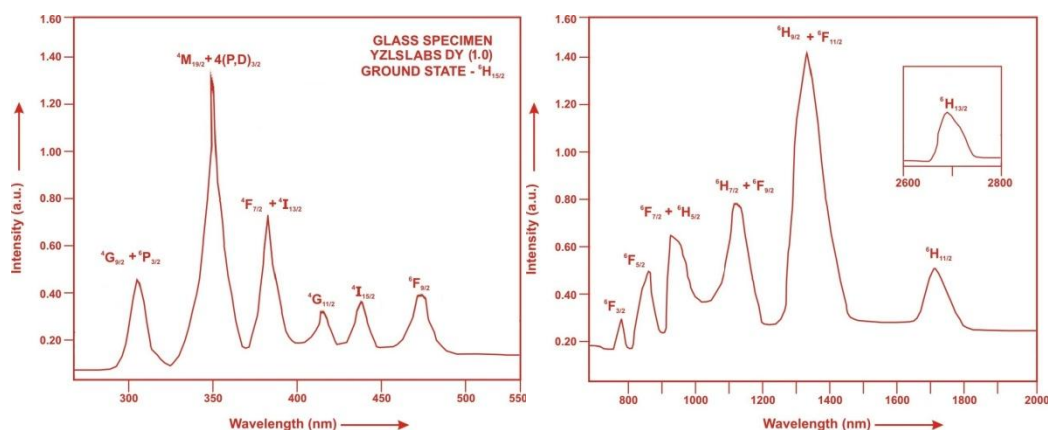


Fig. (4): Absorption spectrum of YZLSLABSDY (1.0) glass.

The experimental and calculated oscillator strength for Dy^{3+} ions in YZLSLABS glasses are given in **Table 3**.

Table 3: Measured and calculated oscillator strength ($P_m \times 10^{-6}$) of Dy^{3+} ions in YZLSLABS glasses.

Energy level from $^6H_{15/2}$	Glass YZLSLABSDY(1.0)		Glass YZLSLABS DY(1.5)		Glass YZLSLABS DY(2.0)	
	$P_{exp.}$	$P_{cal.}$	$P_{exp.}$	$P_{cal.}$	$P_{exp.}$	$P_{cal.}$
$^6H_{13/2}$	4.25	3.29	4.22	3.27	4.18	3.24
$^6H_{11/2}$	3.25	3.49	3.20	3.46	3.15	3.42
$^6H_{9/2}+^6F_{11/2}$	12.25	12.36	12.15	12.28	12.08	12.22
$^6H_{7/2}+^6F_{9/2}$	7.05	6.78	6.98	6.74	6.92	6.70
$^6F_{7/2}+^6H_{5/2}$	6.02	6.27	5.96	6.21	5.91	6.15
$^6F_{5/2}$	3.05	3.23	2.98	3.20	2.93	3.16
$^6F_{3/2}$	1.96	0.61	1.92	0.60	1.87	0.60
$^6F_{9/2}$	2.01	0.49	1.98	0.48	1.92	0.48
$^4I_{15/2}$	2.25	1.26	2.21	1.25	2.15	1.23
$^4G_{11/2}$	1.25	0.11	1.20	0.11	1.16	0.11
$^6F_{7/2}+^4I_{13/2}$	5.85	5.42	5.80	5.38	5.72	5.33
$^6M_{19/2}+4(P,D)_{3/2}$	9.15	9.84	9.11	9.82	9.06	9.81

$^4G_{9/2} \rightarrow ^6P_{3/2}$	3.75	3.36	3.68	3.33	3.62	3.30
r.m.s. deviation	0.8038		0.7880		0.7645	

*Low r.m.s.deviation values clearly indicate the accuracy of fitting.

The values of Judd-Ofelt intensity parameters are given in Table 4.

Table4: Judd-Ofelt intensity parameters for Dy^{3+} doped YZLSLABS glass specimens.

Glass Specimens	$\Omega_2(\text{pm}^2)$	$\Omega_4(\text{pm}^2)$	$\Omega_6(\text{pm}^2)$	Ω_4/Ω_6	Trend	Ref.
YZLSLABSDY (1.0)	3.987	1.017	2.721	0.3738	$\Omega_2 > \Omega_6 > \Omega_4$	P.W.
YZLSLABSDY (1.5)	3.945	1.027	2.689	0.3819	$\Omega_2 > \Omega_6 > \Omega_4$	P.W.
YZLSLABSDY (2.0)	3.913	1.038	2.657	0.3907	$\Omega_2 > \Omega_6 > \Omega_4$	P.W.
ZLACSLBB (HO)	5.939	1.345	2.187	0.6150	$\Omega_2 > \Omega_6 > \Omega_4$	[33].
ABSPLP (DY)	11.930	2.130	2.620	0.8130	$\Omega_2 > \Omega_6 > \Omega_4$	[34].
BBGG (DY)	7.390	1.329	1.468	0.9053	$\Omega_2 > \Omega_6 > \Omega_4$	[35].
LBWB (DY)	5.603	0.851	1.674	0.5084	$\Omega_2 > \Omega_6 > \Omega_4$	[36].

4.5 Excitation Spectrum

The Excitation spectra of Dy^{3+} doped YZLSLABSDY (1.0) glass specimens have been presented in Figure 5 in terms of Excitation Intensity versus wavelength. The excitation spectrum was recorded in the spectral region 315–480 nm fluorescence at 575nm having different excitation band centered at 322, 353, 365, 385, 425, 454 and 473 nm are attributed to the $^6P_{3/2}$, $^6P_{7/2}$, $^4P_{3/2}$, $^4I_{13/2}$, $^4G_{11/2}$, $^4I_{15/2}$ and $^4F_{9/2}$ transitions, respectively. The highest absorption level is $^4I_{13/2}$ and is at 385nm. So this is to be chosen for excitation wavelength.

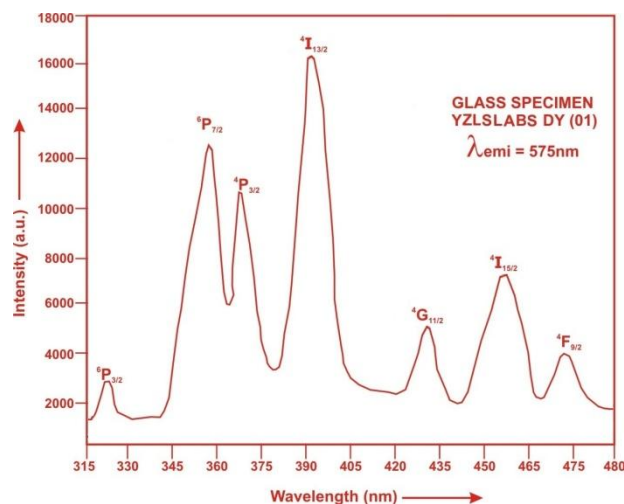


Fig. (5): Excitation spectrum of YZLSLABS DY (1.0) glass.

4.6 Fluorescence Spectrum

The fluorescence spectrum of Dy^{3+} doped in yttrium zinc lithium sodalimealuminoborosilicate glass is shown in Figure 6. There are four broad bands observed in the Fluorescence spectrum of Dy^{3+} doped yttrium zinc lithium sodalimealuminoborosilicate glass. The wavelengths of these bands along with their assignments are given in Table 6. The peak with maximum emission intensity appears at 485nm, 575nm, 665nm and 752 nm and corresponds to the $(^4F_{9/2} \rightarrow ^6H_{15/2})$, $(^4F_{9/2} \rightarrow ^6H_{13/2})$, $(^4F_{9/2} \rightarrow ^6H_{11/2})$ and $^4F_{9/2} \rightarrow ^6H_{9/2}$ transition.

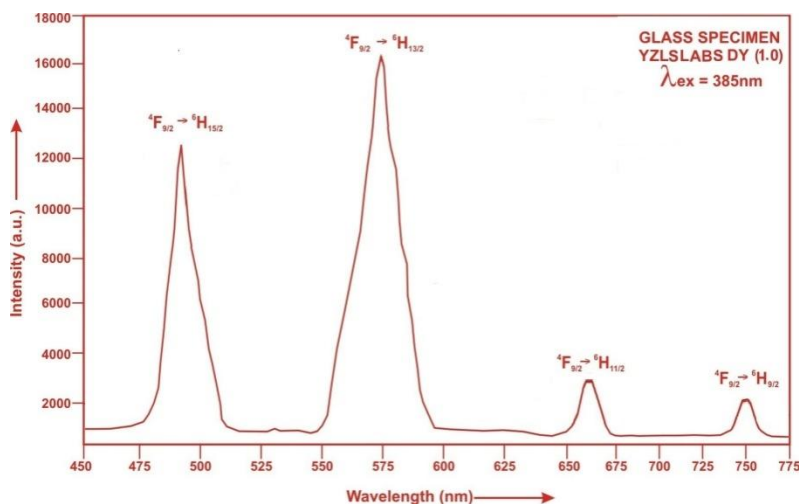


Fig. (6):Fluorescence spectrum of YZLSLABS DY (1.0) glass.

Table5: Emission peak wave lengths (λ_p),radiative transition probability (A_{rad}),branching ratio (β),stimulated emission cross-section(σ_p) and radiative life time(τ_R)for various transitions in Dy^{3+} doped YZLSLABSglasses.

Transition	λ_{max} (nm)	YZLSLABSDY(1.0)					YZLSLABSDY(1.5)					YZLSLABSDY(2.0)			
		$A_{rad}(s^{-1})$	β	σ_p ($10^{-20} cm^2$)	$\tau_R(\mu s)$		$A_{rad}(s^{-1})$	β	σ_p ($10^{-20} cm^2$)	$\tau_R(\mu s)$		$A_{rad}(s^{-1})$	β	$\sigma_p(10^{-20} cm^2)$	$\tau_R(10^{-20} cm^2)$
$4F_{9/2} \rightarrow 6H_{13/2}$	485	137.94	0.2249	0.243	163.04		136.76	0.2248	0.235	164.37		135.59	0.2244	0.227	165.53
$4F_{9/2} \rightarrow 6H_{13/2}$	575	405.20	0.6606	1.480			401.19	0.6606	1.408			399.20	0.6608	1.352	
$4F_{9/2} \rightarrow 6H_{11/2}$	665	40.61	0.0662	0.181			40.29	0.0662	0.175			40.05	0.0663	0.169	
$4F_{9/2} \rightarrow 6H_{9/2}$	752	29.60	0.0483	0.179			29.42	0.0484	0.152			29.28	0.0485	0.147	

V. Conclusion

In the present study, the glass samples of composition $(25-x)SiO_2:10ZnO:10Li_2O:10Na_2O:10K_2O:10Al_2O_3:10Yb_2O_3:15B_2O_3:x Dy_2O_3$. (where $x = 1, 1.5$ and 2 mol %) have been prepared by melt-quenching method. The thermal stability parameter for prepared glass samples are very large. The large thermal parameter indicates that the glass could be easily drawn in to fiber. The value of stimulated emission cross-section (σ_p) is found to be maximum for the transition ($4F_{9/2} \rightarrow 6H_{13/2}$) for all glass specimens. This shows that ($4F_{9/2} \rightarrow 6H_{13/2}$) transition is most probable transition.

References

- [1]. Meena, S.L. (2025). Spectral, Transmittance and Upconversion Properties of Pr^{3+} Doped Bismuth Borate Glasses, *IOSR Appl. Phys.* 17, 20-27.
- [2]. Hegda, V., Vighnesh, K.R., Kamath, S.D., Viswanath, C.S.D., Almuqrin, A.H., Sayyed, M.I., Gangareddy, J., Krishna, R.R., Keshavamurthy, K. (2024). Near-infrared and green emission spectroscopic characteristics of Er^{3+} doped alumina phosphate glasses, *Appl. Phys.* 130: 411, 1-11.
- [3]. Meena, S.L. (2022). Spectral and FTIR Analysis of Ho^{3+} ions doped Zinc Lithium Tungsten Alumino Bismuth borate Glasses, *Int. Eng. Sci. Inv.* 11, 57-63.
- [4]. Klimesz, B., Romanowski, W.R., Lisiecki, R. (2024). Spectroscopic and Thermographic Qualities of Praseodymium-doped Oxyfluorotellurite Glasses, *Molecules*, 29, 3041, 1-13.
- [5]. Fong, W.L., Baki, S.O., Arifin, N.M., Mansor, Y., Nazri, A., Abbas, B.K. (2021). Structural, Thermal and Optical Properties of Rare Earth Doped Lead Tellurite Oxide Glasses, *J. Advan. Res. Fluid Mech. Therm. Sci.* 81, 52-58.
- [6]. Almuqrin, A., Al-Otaibi, J.S., Alwadai, N., Albarzan, B., Shams, M.S., Rammah, Y.S., Elsad, R.A. (2025). Neodymium ion-doped borate-silicate glass: a through analysis for applications in optical and protective radiation, *Eur. Phys. J. Plus*, 140: 259, 1-16.
- [7]. Eales, J.D., Bell, A.M.T., Cutforth, D.A., Kruger, A.A., Bingham, P.A. (2023). Structural changes in borosilicate glasses as a function of Fe_2O_3 content: A multi-technique approach, *J. Non-Cryst. Solids*, 622, 122664.
- [8]. Meena, S.L. (2021). Spectral and Raman Analysis of Nd^{3+} doped Zinc Lithium Sodalime Cadmium Borosilicate Glasses, *Int. J. Chem. Phys.* 10, 8-16.
- [9]. Jaidass, N., Moorthi, C.K., Babu, A.M., Babu, M.R. (2018). Luminescence properties of Dy^{3+} doped lithium zinc borosilicate glasses for photonic applications, *Heliyon*, 4(3), e00555.
- [10]. Kumar, R., Rakesh, R.B., Mhatre, S.G., Bhatia, V., Kumar, D., Singh, H., Singh, S.P., Kumar, A. (2021). Thermoluminescence, structural and optical properties of Ce^{3+} doped borosilicate glasses, *J. Mater. Sci. Mater. Electron.* 32, 18381-18396.
- [11]. Rao, T.G.V.M., Kumar, A.R., Neeraja, K., Veeraiiah, N. and Reddy, M.R. (2013). Optical and structural investigation of Eu^{3+} ions in Nd^{3+} co-doped magnesium lead borosilicate glasses, *J. Alloy. Compd.* 557, 209-217.
- [12]. Muniz, R.F., Zanuto, V.S., Gibin, M.S., Gunha, J.V., Novatski, A., Rohling, J.H., Medina, A.N., Baesso, M.L. (2023). Down and upconversion processes in Nd^{3+}/Yb^{3+} co-doped sodium calcium silicate glasses with concomitant Yb^{2+} assessment, *Appl. Phys. Lett.* 124, 342-348.

- [13]. Hong,Z.,Yue,H.,Gong,G.,Lai,F.,Zou,Z.,You,W.,Wu,S.,Huang,J.(2024). Spectroscopic study of Dy³⁺ ions doped gallium silicate glasses for yellow solid state lasers, *Silicon*, 16,463-470.
- [14]. Meena,S.L.(2021). Spectral and Raman Analysis of Sm³⁺Doped in ZincLithium SodaLimeAluminoSilicate Glasses, *Int.Eng.Sci.Inv.* 4,28-33.
- [15]. Pawar, P.P., Munishwar, S.R. and Gedam, R.S. (2017). Intense white light luminescent Dy³⁺ doped lithium borate glasses for WLED: a correlation between physical, thermal, structural and optical properties. *Solid State Sci.*, 64, 41–50.
- [16]. Rani.P.R.,Venkateswarlu,M.,Swapna,K.,Mahamuda,Sk.,Srinivas Prasad,M.V.V.K.,Rao,A.S.(2020).Spectroscopic and luminescence properties of Ho³⁺ ions doped barium lead aluminofluoro borate glasses for green laser applications,*Solid State Sci.*102,106175.
- [17]. Kotab,I.E.,Okasha,S.Y.,Zidan,N.A.(2023).Extensive study on the optircl and structural characteristics of Nd³⁺ doped lead-borate-strontium-tungsten glass system.*Judd-Ofelt Anal.Res.Chem.*5,1-12.
- [18]. Meena,S.L.(2022).Spectral and Upconversion properties of Eu³⁺ doped in zinc lithium potassiumniobate borosilicate glasses, *Int. J. Res. Appl. Sci. Eng. Tech.*10,62-67.
- [19]. Gautam,C., Yadav,Y.K., Mishra,V.K.,Vikram,K.(2012). Synthesis, IR and Raman Spectroscopic Studies of (Ba,Sr)TiO₃ Borosilicate Glasses with Addition of La₂O₃, *Open J.Inorg. Non-meta. Mat.* 2012, 2, 47-54
- [20]. Bruns,S.,Uesbeck,T.,Weil,D.(2020). Influence of Al₂O₃Addition on Structure and Mechanical Properties of Borosilicate Glasses,*Front.Mater.*7:789,1-14.
- [21]. Hathot,S.F.,Al Dahhagh,B.M.,Aboud,H(2024). Structural and spectroscopic correlation in barium-boro-tellurite glass hosts: effects of Dy₂O₃ doping, *Chal.Lett.*21, 201-215.
- [22]. Liu,Y.,Wang,Y.,Wang,M.,Shen,H.,Huang,C.,Wang,X.,Gao,J.,Tu,C.(2023).Structure and Spectral properties of Dy³⁺ doped CaYAlO₄ single crystal,*Scient.Reports*,13:6066.
- [23]. Jimenez,J.A.,Hedge,V.,Viswanath,C.S.D.,Amesimenu,R.(2024).Insights into the Structural, Thermal/Dilatometric, and Optical Properties of Dy³⁺-Doped Phosphate Glasses for Lighting Applications,*ACS Phys.Chem.Au*,4,720-735.
- [24]. Hathot,S.F.,Dabbagh,B.M.A.,Aboud,H.(2025). Structural and Optical properties of novel borotellurite glass-ceramic with composition B₂O₃- TeO₂-BaO-Dy₂O₃, *Journal of Physics: Conf. Series*, 2974,1-16.
- [25]. Meena,S.L.(2024).Spectral and Thermal properties of Tm³⁺doped in zinc lithium tungsten antimonyborophosphate glasses, *IOSR Appl.Phys.*16,10-15.
- [26]. Meena,S.L.(2025).Spectral and Thermal properties of Eu³⁺ doped ytteriumzinc lithium alumina tungsten potassiumniobatebismuth borate blasses with low Hruby's criterion, *IOSR Appl.Phys.*17,48-54.
- [27]. Judd, B.R.(1962).Optical absorption intensities of rare earth ions,*Phys.Rev.*127,750-761.
- [28]. Ofelt, G.S. (1962). Intensities of crystal spectra of rare earth Ions, *Chem.Phys*37, 511-520.
- [29]. Rojas,S.S.,Souza,J.E.,Yukimitu,Hernandes,A.C.(2014).Structural,thermal and optical properties of CaBO and CaLiBO glasses doped with Eu³⁺,*J.Non-Cryst.Solids*,398-399,57-61.
- [30]. Meena,S.L.(2025).Spectral,Thermal and Raman Analysis of Ho³⁺ doped Boro phosphate glasses with large Balaji Parameter,*IOSR Appl.Phys.*17,24-31.
- [31]. Meena,S.L.(2024).Spectral, Thermal and FTIR analysis of Pr³⁺doped in Zinc Lithium Sodium Lead Tungsten Aluminophosphate glasses,*Int. J.Innov.Res.Sci. Eng. Tech.*13,235-244.
- [32]. Shwetha,M.,Eraiah,B.(2019).Influence of Er³⁺ ions on the physical,structural,optical and thermal properties of ZnO-Li₂O-P₂O₅ glasses,*App.Phys.*221,1-11.
- [33]. Meena,S.L.(2025). Spectroscopic and Photoluminescence Properties of Ho³⁺-doped Borate Glasses with NIR Light Emission Applications,*IOSR Appl.Phys.*17,34-40.
- [34]. Babu,S.,Prasad,V.R.,Rajesh,D.,Ratnakaram,Y.C.(2015).Luminescence properties of Dy³⁺ doped different fluoro-phosphate glasses for solid state lighting applications,*J.Mol.Struct.*1080,153-161.
- [35]. Pisarski,W.A.(2022).Judd-Ofelt Analysis and Emission Properties of Dy³⁺ ions in Borogermanate Glasses,*Materials*,15,9042,1-18.
- [36]. Ram,P.S,Babu,Y.N.Ch.R.,Kumar,M.K.,Kumar,A.S.(2014). Spectral Studies of Dy³⁺ Doped Heavy Metal Oxide Glasses, *Int. J. Current Eng. Tech.*4, 3473-3479